



NIH Public Access

Author Manuscript

AJNR Am J Neuroradiol. Author manuscript; available in PMC 2010 February 12.

Published in final edited form as:

AJNR Am J Neuroradiol. 2010 February ; 31(2): 347. doi:10.3174/ajnr.A1809.

Combining MRI, PET and CSF biomarkers in diagnosis and prognosis of Alzheimer's disease

KB Walhovd^{1,2}, AM Fjell^{1,2}, J Brewer^{3,5}, LK McEvoy³, C Fennema-Notestine^{3,4}, DJ Hagler Jr³, RG Jennings³, D Karow³, AM Dale^{3,5}, and The Alzheimer's Disease Neuroimaging Initiative

¹Center for the Study of Human Cognition, Department of Psychology, University of Oslo, Oslo, Norway

²Department of Neuropsychology, Ulleval University Hospital, Oslo, Norway

³Department of Radiology, University of California, San Diego, La Jolla, CA

⁴Department of Psychiatry, University of California, San Diego, La Jolla, CA

⁵Department of Neuroscience, University of California, San Diego, La Jolla, CA

Abstract

Background and purpose—To combine MRI, FDG-PET and CSF biomarkers in diagnostic classification and two year prognosis of Mild Cognitive Impairment (MCI) and Alzheimer's disease (AD), examining: 1) which measures are most sensitive to diagnostic status? 2) to what extent do the methods provide unique information in diagnostic classification 3) which measures are most predictive of clinical decline?

Materials and Methods—Alzheimer's Disease Neuroimaging Initiative baseline MR, FDG-PET and CSF data from 42 controls, 73 MCI and 38 AD patients and two year clinical follow up data for 36 controls, 51 MCI, and 25 AD patients were analyzed. The hippocampus, entorhinal, parahippocampal, retrosplenial, precuneus, inferior parietal, supramarginal, middle temporal, lateral and medial orbitofrontal cortices were used as regions of interest. CSF variables included $\alpha\beta42$, t-tau, p-tau, and ratios of t-tau/ $\alpha\beta42$ and p-tau/ $\alpha\beta42$. Regression analyses were performed to determine measures' sensitivity to diagnostic status as well as two year change in Clinical Dementia Rating sum of boxes (CDR-SB), Mini Mental Status Exam (MMSE), and delayed logical memory in MCI.

Results—Hippocampal volume, retrosplenial thickness and t-tau/ $\alpha\beta42$ uniquely predicted diagnostic group. Change in CDR-SB was best predicted by retrosplenial thickness, MMSE by retrosplenial metabolism and thickness, and delayed logical memory by hippocampal volume.

Conclusion—All biomarkers were sensitive to diagnostic group. Combining MR morphometry and CSF biomarkers improved diagnostic classification (controls vs. AD). MR morphometry and PET were largely overlapping in value for discrimination. Baseline MR and PET measures were more predictive of clinical change in MCI than were CSF measures.

*Address correspondence to: Kristine B. Walhovd, Dept of Psychology, University of Oslo, Pb. 1094 Blindern, 0317 Oslo, Norway, phone: k.b.walhovd@psykologi.uio.no.

** Data used in the preparation of this article were obtained from the Alzheimer's Disease Neuroimaging Initiative (ADNI) database (www.loni.ucla.edu/ADNI). As such, the investigators within the ADNI contributed to the design and implementation of ADNI and/or provided data but did not participate in analysis or writing of this report. A complete listing of ADNI investigators is available at http://www.loni.ucla.edu/ADNI/Data/ADNI_Authorship_List.pdf

Introduction

Multiple biomarkers have proven sensitive to Alzheimer's disease (AD) and Mild Cognitive Impairment (MCI), a potential prodromal stage of AD. These include patterns of regional cerebral atrophy and hypometabolism detected by MRI and fluorodeoxyglucose (FDG) PET (1), and quantification of specific proteins in CSF, including tau protein and $\alpha\beta42$ (2). Tau is associated with axonal microtubules and is the main structural element of neurofibrils in AD. High CSF tau levels probably reflect axonal degeneration (3). $\alpha\beta42$ is derived from cleavage of amyloid precursor protein, and CSF $\alpha\beta42$ levels are lowered early in AD, possibly due to sequestering of $\alpha\beta42$ in neuritic plaques (4). A full spectrum of imaging and CSF analysis methods is seldom employed, limiting knowledge on how they may best be combined. The Alzheimer's Disease Neuroimaging Initiative (ADNI), a large multi-site study, was launched to enable analyses of combinations of different candidate biomarkers for AD.

Recent findings indicate that MRI can be used to quantify regional atrophy in MCI distinguishing early and later preclinical stages of AD (5), and such measures are predictive of clinical decline across one year (6–8). A pattern of parietotemporal metabolic reductions in MCI and AD, and frontal metabolic reductions later in the disease, has been established through the last decades of research (1,9,10) and has recently been confirmed in ADNI PET data (11). The relative sensitivity of FDG-PET and MR morphometry to AD-related changes is, however, not well established. It has been assumed that metabolic changes associated with neocortical dysfunction may be detectable by FDG-PET before atrophy appears. Consistent with this, De Santi et al. (12) reported that metabolism reductions exceeded volume losses in MCI, and Mosconi et al (13) found the same in presymptomatic early-onset familial AD. However, Jagust et al. (14) found that cingulate hypometabolism was a significant risk factor in addition to MR measures of hippocampal atrophy, but the latter was a more statistically robust risk factor in a group of cognitively impaired but not demented (CIND) elderly (15). Different brain characteristics relevant for the understanding MCI and AD may be captured by FDG-PET and MR morphometry. For instance, a report based on ADNI data has indicated that FDG-PET and MRI measures may be complementary and differentially sensitive to memory in health and disease, with metabolism being the stronger predictor in normal controls, and morphometry most related to memory function in AD (16). As for CSF-MRI relations, recent reports (17–22) indicate that cerebral anatomical differences are related to tau and $\alpha\beta42$ and behavioral cognitive measures in AD and MCI. However, MRI and CSF biomarkers have not simultaneously been related and compared to information obtained by FDG-PET. It is important to test the specific sensitivity of all biomarkers simultaneously to be able to optimize the combination of measures in diagnosis and prognosis. We investigated 1) Which methods are the most sensitive to established AD-related pathology? 2) To what extent do the methods provide unique vs. overlapping information? 3) Which methods are the most predictive of clinical decline across two years?

Methods

The raw data used in the preparation of this article were obtained from the Alzheimer's Disease Neuroimaging Initiative (ADNI) database (www.loni.ucla.edu/ADNI). ADNI was launched in 2003 by the National Institute on Aging (NIA), the National Institute of Biomedical Imaging and Bioengineering (NIBIB), the Food and Drug Administration (FDA), private pharmaceutical companies and non-profit organizations. The primary goal of ADNI has been to test whether serial MRI, PET, other biological markers, and clinical and neuropsychological assessment can be combined to measure the progression of MCI and early AD. The Principal Investigator of this initiative is Michael W. Weiner, VA Medical Center and University of California – San Francisco. There are many co-investigators, and subjects have been recruited from over 50 sites across the U.S. and Canada. The ADNI has recruited 229 healthy elderly,

398 MCI and 192 AD patients to participate and be followed for 2–3 years. For up-to-date information see www.adni-info.org.

Sample

ADNI eligibility criteria are described at http://www.adni-info.org/index.php?option=com_content&task=view&id=9&Itemid=43. Briefly, participants are 55–90 years of age, had an informant providing an independent evaluation of functioning, and spoke English or Spanish. Subjects were willing and able to undergo test procedures including neuroimaging and longitudinal follow up, and all gave informed consent. Specific psychoactive medications are excluded. General inclusion/exclusion criteria of the ADNI study are as follows: 1. Normal subjects: Mini-Mental State Examination (MMSE) (23) scores between 24–30 inclusive (no person enrolled as an NC in the present sample had an MMSE score below 26), Clinical Dementia Rating (CDR) of 0, non-depressed, non-MCI, and nondemented. 2. MCI subjects: MMSE scores between 24–30, inclusive (exceptions made on a case by case basis, but no such exceptional cases were enrolled as MCI patients in the present sample), a memory complaint, objective memory loss measured by Wechsler Memory Scale Logical Memory II, CDR of 0.5, absence of significant levels of impairment in other cognitive domains, essentially preserved activities of daily living, and an absence of dementia. 3. Mild AD: MMSE scores between 20–26 (inclusive; exceptions made on a case by case basis), CDR of 0.5 or 1.0, and meets NINCDS/ADRDA criteria for probable AD. Only ADNI subjects for whom adequate processed and quality checked MRI, FDG-PET and CSF baseline data were available were included. This yielded a total of 153 participants. Demographics are shown in Table 1.

Standard protocol approvals, registrations and patient consents

The protocol was approved by the institutional review boards of participating sites. Written informed consent was obtained from all subjects, or from guardians of patients.

MR acquisition and analysis

All scans used here were from 1.5 T scanners. Data were collected across a variety of scanners with protocols individualized for each scanner, as defined at <http://www.loni.ucla.edu/ADNI/Research/Cores/index.shtml>, and processed as described elsewhere (5,16). Briefly, raw DICOM MRI scans (including two T1-weighted volumes per case) were downloaded from the ADNI site (<http://www.loni.ucla.edu/ADNI/Data/index.shtml>), reviewed for quality, automatically corrected for spatial distortion due to gradient nonlinearity (24) and B1 field inhomogeneity (25), registered, and averaged to improve signal-to-noise. Scans were segmented as described by Fischl et al. (26), yielding volumetric data for the hippocampal formation (consisting of the dentate gyrus, CA fields, subiculum/ parasubiculum and the fimbria (27)). The procedure (26,28) uses a probabilistic atlas and applies a Bayesian classification rule to assign a neuroanatomical label to each voxel. The cortical surface was reconstructed to measure thickness at each surface point using a semi-automated approach described elsewhere (29–34). Thickness measurements were obtained by reconstructing representations of the gray/white matter boundary (29,30) and the pial surface and then calculating the distance between those surfaces at each point across the cortical mantle. The measurement technique used here has been validated via histological (35) as well as manual measurements (36). The entire cortical surface was parcellated into numerous cortical areas (28,37). To limit multiple comparisons, candidate regions of interest (ROIs) were selected based on previous MRI and PET findings (1,5,7,16,38–43) indicating sensitivity to AD-related pathology: The hippocampi, entorhinal, parahippocampal, retrosplenial, precuneus, inferior parietal, supramarginal, middle temporal, lateral and medial orbitofrontal gyri. In the parcellation

method used here (37), the entire cingulate cortex is defined and divided into four separate regions, including rostral and caudal anterior cingulate, posterior cingulate, and isthmus cingulate, the latter referred to here as retrosplenial cortex for consistency with other published studies (5,16,38). The retrosplenial region may also be referred to as the isthmus of the cingulate or caudal posterior cingulate area in other contexts. For a depiction of the exact ROIs used, see Figure 1.

FDG-PET acquisition and analysis

Subjects were scanned after a 4 hour fast (water only). Plasma glucose had to be ≤ 180 mg/dL for FDG to be injected. An intravenous catheter was placed in one arm for injection of [18F] FDG. Imaging began at 30 min post injection, and the scan was acquired as six 5-min frames. For each subject, FDG-PET frames were averaged and registered to the corresponding distortion-corrected and intensity-normalized MRI volume. PET activity for each subject was sampled onto their reconstructed cortical surface, averaged within each ROI and normalized to activity within the pons (44).

CSF acquisition and analysis

CSF samples obtained by lumbar puncture were examined for t-tau, p-tau and $\alpha\beta42$ using an immunoassay method (45). The measurements were performed by Drs. L. Shaw and J. Trojanowski of the ADNI Biomarker Core at the University of Pennsylvania School of Medicine. The CSF biomarkers analysed in the present paper include beta amyloid 1–42 ($\text{A}\beta42$; M and SDs: 202 (56), 159 (51), 136 (39) pg/mL for NC, MCI and AD respectively), tau protein (t-tau; M and SDs: 68 (28), 100 (65), 125 (67) pg/mL for NC, MCI and AD respectively), and phosphorylated-tau protein 181 (p-tau; M and SDs: 26 (17), 36 (19), 45 (23) for NC, MCI and AD respectively). The ratio of tau and $\text{A}\beta42$ (tau/ $\text{A}\beta42$; M and SDs: 37 (.21), .74 (.67), .98 (.56) for NC, MCI and AD respectively), and p-tau $\text{A}\beta42$ ratio (p-tau/ $\text{A}\beta42$; M and SDs: .16 (.16), .26 (.19), .36 (.22) for NC, MCI and AD respectively) were also included. A one-way ANOVA on the residual CSF values after age and sex were regressed out showed significant ($p < .001$) main effects of group on all variables. Post hoc tests controlling for multiple comparisons showed significant ($p < .05$) differences between NC and MCI, NC and AD, and MCI and AD, with a few exceptions where trends ($p < .10$) were observed (difference in t-tau between MCI and AD, p-tau between NC and MCI, and t-tau/ $\text{A}\beta42$ between MCI and AD).

Clinical and cognitive measures

Change scores were calculated by subtracting baseline scores from scores obtained at the two-year follow up. In addition to CDR-SB (46) and MMSE (23), delayed recall on the Wechsler Logical Memory Test (47) was included. This test requires the subject to recall a story read by the examiner after a 30–40 minute delay, and is sensitive to the episodic memory deficits in MCI.

Statistics

A repeated measures general linear model with the ten ROIs \times hemisphere (left, right) \times diagnostic group (NC, MCI, AD) with age and sex as covariates, showed no significant effect of hemisphere across ROIs ($F[1,148] = 1.530$, $p = .218$) and no interaction of hemisphere \times diagnostic group ($F[2,148] = .847$, $p = .431$). Hence, values were averaged across hemispheres, effects of age and sex regressed out, and the standardized residuals were used in the analyses. Correlation analyses with MR, FDG-PET and CSF measures were run to assess their covariance. To select the measures yielding the most explained variance for each method, the values were entered in three separate logistic stepwise regressions using MR, PET and CSF measures respectively, predicting NC vs. AD. The selected MR, PET and CSF variables were

then entered simultaneously in multi-method stepwise logistic regression analyses predicting NC vs. AD, and NC vs. MCI. Next, the variables identified by the NC vs. AD classification analysis were correlated with two year follow up CDR-SB, MMSE, and delayed logical memory change scores in the MCI group, and were entered as predictors in stepwise regression analyses with the respective behavioral change scores as the dependent variables.

Results

Correlation analyses in the MCI group for morphometry and metabolism for the 10 ROIs and the five CSF variables showed no significant ($p < .05$, corrected for 10 ROI comparisons) correlations among CSF variables and morphometry or metabolism in any ROI, whereas moderate correlations were found between morphometric and metabolic measures for hippocampus, entorhinal, retrosplenial and inferior parietal regions (see Supplemental Table 1).

Table 2 shows results of the separate logistic stepwise regressions predicting NC vs. AD classification based on MRI, FDG-PET and CSF measures. For MRI, hippocampal volume, entorhinal and retrosplenial thickness were included in the final model, yielding an overall classification accuracy of 85.0%, and about 71 % explained variance (Nagelkerke R^2). For FDG-PET, entorhinal, retrosplenial and lateral orbitofrontal metabolism were included in the final model, yielding an overall classification accuracy of 82.5%, and about 62 % explained variance. For CSF, the ratio of t-tau/ $\alpha\beta42$ was the single unique predictor, yielding an overall classification accuracy of 81.2%, and about 52 % explained variance. Thus, hippocampal volume, entorhinal and retrosplenial thickness, entorhinal, retrosplenial and lateral orbitofrontal metabolism, and t-tau/ $\alpha\beta42$ ratio were entered in a logistic regression analysis to classify NC vs. AD, and the results are shown in Table 3.

In the final model, hippocampal volume, retrosplenial thickness and t-tau/ $\alpha\beta42$ -ratio were included as predictors, yielding an overall classification accuracy of 88.8%, and about 78 % explained variance. Figure 2 depicts the receiver operating characteristics (ROC) curves for these variables when using one (hippocampal volume), vs a combination of two (hippocampal volume and t-tau/ $\alpha\beta42$ -ratio) and all three variables (hippocampal volume, t-tau/ $\alpha\beta42$ -ratio and retrosplenial thickness) shown to be unique predictors of normal control vs Alzheimer's disease classification. Predicted values from logistic regressions were used for calculation of the ROC curves. Statistical comparisons of the areas under the curve (AUC) of these classifiers were performed by using the method of Hanley and McNeil (48). This approach yielded a significant difference ($p < .05$) between the AUC when using hippocampal volume alone vs when using hippocampal volume and t-tau/ $\alpha\beta42$ -ratio in combination, and hippocampal volume, t-tau/ $\alpha\beta42$ -ratio and retrosplenial thickness in combination. The difference of the AUCs when using hippocampal volume and t-tau/ $\alpha\beta42$ -ratio vs hippocampal volume, t-tau/ $\alpha\beta42$ -ratio and retrosplenial thickness in combination was clearly smaller and not significant ($p > .05$). Note however, that all meaningful differences in AUC e.g. in terms of sensitivity vs specificity, causing the curves to cross, may not necessarily be captured as statistically significant. The same set of predictor variables were entered in an analysis to predict diagnostic classification for NC and MCI, which revealed that hippocampal volume and t-tau/ $\alpha\beta42$ -ratio were unique predictors, yielding an overall classification accuracy of 79.1%, and about 40 % explained variance.

Table 4 shows correlations for each variable included in the regression models and the cognitive change scores (CDR-SB, MMSE, delayed logical memory). In MCI, baseline retrosplenial thickness correlated with two year change in CDR-SB and MMSE, where thicker cortex was associated with less CDR-SB elevation and less MMSE reduction. Retrosplenial and entorhinal metabolism correlated negatively with MMSE change. Hippocampal volume correlated

positively with delayed logical memory. There were no significant correlations with clinical change measures for t-tau/αβ42 in MCI. T-tests of the Fischer z-transformed correlation coefficients showed that the T-tau/αβ42 ratio correlated significantly lower ($p < .05$) with CDR-SB and MMSE change than did retrosplenial thickness; and significantly lower with MMSE change than did entorhinal and retrosplenial metabolism. Lateral orbitofrontal metabolism also correlated significantly lower with change in CDR-SB and delayed logical memory than did retrosplenial thickness and hippocampal volume.

In the stepwise regression analysis predicting CDR-SB change, only retrosplenial cortical thickness was included as a unique predictor ($y = 1.231 - 0.731x$, $p = .002$), explaining 18% of the variance. In predicting MMSE change, retrosplenial metabolism was included in the first step ($y = -1.193 + 1.534 x_1$, $p = .002$ for x_1 , $R^2 = .22$), and retrosplenial thickness was added in the second ($y = -1.197 + 1.177x_1 + 0.776 x_2$, $p = .009$ for x_1 and $.042$ for x_2 , $R^2 = .29$). Only hippocampal volume was included as a predictor of delayed logical memory change ($y = 0.240 + 1.669 x_1$, $p = .003$ for x_1 , $R^2 = .17$). The regression plots for CDR-SB and MMSE change predicted from retrosplenial thickness and metabolism, and delayed logical memory predicted from hippocampal volume, are shown in Figure 3. There was one outlier for the MMSE change score, with a 13 point decline. Without this outlier, only retrosplenial metabolism was included in the model for predicting MMSE change ($y = -1.023 + 1.091 x_1$, $p = .004$ for x_1 , $R^2 = .16$), but a trend was observed for retrosplenial thickness ($p = .079$).

Discussion

Morphometry, metabolism and CSF biomarkers were all sensitive to diagnostic status. The best classification accuracy of NC vs. AD was obtained by MRI morphometry measures (hippocampal volume, entorhinal and retrosplenial cortical thickness). However, classification accuracies close to those obtained by MRI were also obtained by FDG-PET (entorhinal, retrosplenial and lateral orbitofrontal metabolism) and CSF measures (T-tau/ αβ42-ratio). In the multi-modal analysis, FDG-PET measures appeared to provide largely redundant information, whereas hippocampal volume, retrosplenial thickness and the t-tau/αβ42 ratio were unique predictors of diagnostic status. In particular, the inclusion of the CSF biomarker in addition to MR hippocampal volume did result in a significant improvement in classification in terms of area under the curve. Thus, the combination of MR morphometry and CSF biomarkers yielded the highest diagnostic classification accuracy. Contrary to this, in prediction of clinical change over two years, FDG-PET and MRI morphometry were the best predictors. However, with the exception of retrosplenial metabolism and thickness in the prediction of change in MMSE scores, the two measures were largely redundant. Thus, it seems that the benefits of including both MRI morphometry and FDG-PET are modest in predicting clinical decline in MCI.

Whereas CSF biomarkers added to diagnostic accuracy at baseline, they did not predict two year clinical decline in the current MCI group. This may be somewhat surprising since previous studies have found decreased CSF αβ42 and/or tau or tau/αβ42 levels to be predictive of future dementia in MCI patients (2). Several factors may have contributed to discrepancies. First, the ongoing ADNI study may have a more heterogeneous MCI group than some of the previously published CSF studies. As pointed out by Hansson and colleagues (49), participants included in CSF studies have generally been highly selected, for example, by inclusion of only MCI patients that progress to AD. In ADNI, the ultimate end-point is not known for many MCI patients. Further, studies have often employed dichotomized variables for CSF values and prognosis (49,50). A stable/conversion dichotomization involves clinical judgment, which may vary from physician to physician, and demands long follow-up intervals impractical for clinical trials. It may be advantageous to identify other pre-selection criteria, biomarkers or clinical measures of decline than conversion. In light of this, it is important to relate the biomarkers to

easily administered continuous behavioral measures. Interestingly, another study investigating continuous variables (51) did not find any association between MMSE change and change in CSF levels of either $\text{A}\beta 42$, tau or p-tau ($r = .18, -.03$, and $-.07$, respectively). This does not mean that CSF measures are not related to clinical change. CSF tau/ $\text{A}\beta 42$ ratio did correlate in the expected negative direction with change in logical delayed memory in the present sample, but the effect size was too modest to reach significance. Select MR morphometry and FDG-PET measures at baseline were significantly more sensitive to two year change in CDR-SB and MMSE than were CSF measures. Both cortical thickness and metabolism of parietal ROIs served as unique predictors of clinical decline, indicating that even though FDG-PET did not contribute uniquely to diagnostic classification when MR morphometric variance was accounted for, some additional prognostic information can be obtained by combining the two imaging modalities.

While the present findings show that the different biomarkers all were sensitive to diagnostic group, a question of great interest is whether the findings regarding specific measures can be applied on an individual subject basis. McEvoy et al. (7) recently reported that semiautomated *individually specific* quantitative MR imaging methods identical to those employed here can be used to identify a pattern of atrophy in MCI that is predictive of conversion to AD after 1 year. Hence, in light of the present findings indicating also somewhat superior sensitivity of such MR morphometry measures compared to other biomarkers, it does seem that these measures are prime candidates to be used on an individual basis e.g. to enrich clinical trials. However, as seen from Figure 3, while the MR morphometry measures evaluated here do predict two year change in screening and memory parameters among MCI patients, the regression plots also show considerable scatter. Hence, while these measures can yield individual prognostic information, this will be associated with considerable uncertainty and at present any such estimate must be made with great caution.

The present results are limited by a number of factors: Participants were selected based on willingness and ability to undergo MR and PET scanning and lumbar puncture, and may thus not be fully comparable to other samples. However, imaging is an integral part of the ADNI protocol, so participants did enter with the intention of having brain scans performed and about half of the ADNI participants have also agreed to have CSF samples drawn (52). In terms of age, MMSE score, $\text{A}\beta 42$, t-tau, p-tau and ratios of t-tau/ $\text{A}\beta 42$ and p-tau/ $\text{A}\beta 42$, the subgroups studied in the present paper do appear to be representative of the larger ADNI sample. The mean values for these indices in the present sample appear very similar to those reported by Shaw et al. (52) for 410 participants with CSF measures, and all the present mean values for age, MMSE, and CSF measures for NC, MCI and AD and deviate less than 1/5 of the standard deviations from the means reported by Shaw et al. (52) for the larger groups.

Still, the present sample may of course not be fully representative of the general population. Further, the multi-site design of the ADNI is likely to add some noise in data collection. Finally, the ADNI study is still ongoing, and the ultimate status of the current MCI group is unknown. That being said, the present study involving multiple-sites and two years of follow-up likely represents a more realistic model for current clinical trial designs than longer interval, single-site studies.

Conclusion

Each of the biomarkers demonstrated potential to inform diagnosis and/ or prognosis and enrich clinical trials. As a single classifier, MR morphometry (hippocampal volume) was the most sensitive to diagnostic group, but the inclusion of CSF biomarkers (t-tau/ $\text{A}\beta 42$) did result in significant improvement of classification (NC/AD). Still, both quantitative MRI morphometry and regional metabolism as assessed by co-registered FDG-PET data provided better prediction of clinical decline than did CSF biomarkers. MRI morphometry showed somewhat superior

diagnostic and prognostic sensitivity and is the least invasive, less expensive and most widely available method. MRI scans are often routinely required as part of the diagnostic work-up, so a broader application of MRI morphometry may be feasible and useful.

Supplementary Material

Refer to Web version on PubMed Central for supplementary material.

Acknowledgments

This work was supported by grants from the National Center for Research Resources (U24 RR021382 - CFN, AMD, DJH) and the National Institute on Aging (R01AG22381 - CFN, LKM, AMD; K01AG029218 – LKM). The work of Walhovd and Fjell was supported by the Norwegian Research Council. Data collection and sharing for this project was funded by the Alzheimer's Disease Neuroimaging Initiative (ADNI; Principal Investigator: Michael Weiner; NIH grant U01 AG024904). ADNI is funded by the National Institute on Aging, the National Institute of Biomedical Imaging and Bioengineering (NIBIB), and through generous contributions from the following: Pfizer Inc., Wyeth Research, Bristol-Myers Squibb, Eli Lilly and Company, GlaxoSmithKline, Merck & Co. Inc., AstraZeneca AB, Novartis Pharmaceuticals Corporation, Alzheimer's Association, Eisai Global Clinical Development, Elan Corporation plc, Forest Laboratories, and the Institute for the Study of Aging, with participation from the U.S. Food and Drug Administration. Industry partnerships are coordinated through the Foundation for the National Institutes of Health. The grantee organization is the Northern California Institute for Research and Education, and the study is coordinated by the Alzheimer's Disease Cooperative Study at the University of California, San Diego. ADNI data are disseminated by the Laboratory of Neuro Imaging at the University of California, Los Angeles.

References

1. Mosconi L, Brys M, Glodzik-Sobanska L, De Santi S, Rusinek H, de Leon MJ. Early detection of Alzheimer's disease using neuroimaging. *Exp Gerontol* 2007;42:129–138. [PubMed: 16839732]
2. Craig-Schapiro R, Fagan AM, Holtzman DM. Biomarkers of Alzheimer's disease. *Neurobiol Dis*. 2008
3. Blennow K, Wallin A, Agren H, Spenger C, Siegfried J, Vanmechelen E. Tau protein in cerebrospinal fluid: a biochemical marker for axonal degeneration in Alzheimer disease? *Mol Chem Neuropathol* 1995;26:231–245. [PubMed: 8748926]
4. Andreasen N, Blennow K. Beta-amyloid (Abeta) protein in cerebrospinal fluid as a biomarker for Alzheimer's disease. *Peptides* 2002;23:1205–1214. [PubMed: 12128078]
5. Fennema-Notestine C, Hagler DJ Jr. McEvoy LK, et al. Structural MRI biomarkers for preclinical and mild Alzheimer's disease. *Hum Brain Mapp*. 2009 In press.
6. Leow AD, Yanovsky I, Parikhshak N, et al. Alzheimer's disease neuroimaging initiative: a one-year follow up study using tensor-based morphometry correlating degenerative rates, biomarkers and cognition. *Neuroimage* 2009;45:645–655. [PubMed: 19280686]
7. McEvoy LK, Fennema-Notestine C, Roddey JC, et al. Alzheimer disease: quantitative structural neuroimaging for detection and prediction of clinical and structural changes in mild cognitive impairment. *Radiology* 2009;251:195–205. [PubMed: 19201945]
8. Misra C, Fan Y, Davatzikos C. Baseline and longitudinal patterns of brain atrophy in MCI patients, and their use in prediction of short-term conversion to AD: results from ADNI. *Neuroimage* 2009;44:1415–1422. [PubMed: 19027862]
9. Mosconi L, Tsui WH, Herholz K, et al. Multicenter standardized 18F-FDG PET diagnosis of mild cognitive impairment, Alzheimer's disease, and other dementias. *J Nucl Med* 2008;49:390–398. [PubMed: 18287270]
10. de Leon MJ, Ferris SH, George AE, et al. Computed tomography and positron emission transaxial tomography evaluations of normal aging and Alzheimer's disease. *J Cereb Blood Flow Metab* 1983;3:391–394. [PubMed: 6603463]
11. Langbaum JBS, Chen K, Lee W, et al. Categorical and correlational analyses of baseline fluorodeoxyglucose positron emission tomography images from the Alzheimer's Disease Neuroimaging Initiative. *Neuroimage*. 2009 In press.
12. De Santi S, de Leon MJ, Rusinek H, et al. Hippocampal formation glucose metabolism and volume losses in MCI and AD. *Neurobiol Aging* 2001;22:529–539. [PubMed: 11445252]

13. Mosconi L, Sorbi S, de Leon MJ, et al. Hypometabolism exceeds atrophy in presymptomatic early-onset familial Alzheimer's disease. *J Nucl Med* 2006;47:1778–1786. [PubMed: 17079810]
14. Jagust WJ, Eberling JL, Wu CC, et al. Brain function and cognition in a community sample of elderly Latinos. *Neurology* 2002;59:378–383. [PubMed: 12177371]
15. Wu CC, Mungas D, Petkov CI, et al. Brain structure and cognition in a community sample of elderly Latinos. *Neurology* 2002;59:383–391. [PubMed: 12177372]
16. Walhovd KB, Fjell AM, Dale AM, et al. Multi-modal imaging predicts memory performance in normal aging and cognitive decline. *Neurobiol Aging*. 2009 In press.
17. de Leon MJ, Mosconi L, Blennow K, et al. Imaging and CSF studies in the preclinical diagnosis of Alzheimer's disease. *Ann N Y Acad Sci* 2007;1097:114–145. [PubMed: 17413016]
18. de Leon MJ, DeSanti S, Zinkowski R, et al. Longitudinal CSF and MRI biomarkers improve the diagnosis of mild cognitive impairment. *Neurobiol Aging* 2006;27:394–401. [PubMed: 16125823]
19. Chou YY, Lepore N, Avedissian C, et al. Mapping correlations between ventricular expansion and CSF amyloid and tau biomarkers in 240 subjects with Alzheimer's disease, mild cognitive impairment & elderly controls. *Neuroimage*. 2009
20. Leow AD, Yanovsky I, Parikhshak N, et al. Alzheimer's Disease Neuroimaging Initiative: A one-year follow up study using tensor-based morphometry correlating degenerative rates, biomarkers and cognition. *Neuroimage*. 2009 In press.
21. Schuff N, Woerner N, Boreta L, et al. MRI of hippocampal volume loss in early Alzheimer's disease in relation to ApoE genotype and biomarkers. *Brain*. 2009
22. Fjell AM, Walhovd KB, Amlien I, et al. Morphometric Changes in the Episodic Memory Network and Tau Pathologic Features Correlate With Memory Performance in Patients With Mild Cognitive Impairment. *American Journal of Neuroradiology* 2008;29:1–7. [PubMed: 18192342]
23. Folstein MF, Folstein SE, McHugh PR. "Mini-mental state". A practical method for grading the cognitive state of patients for the clinician. *J Psychiatr Res* 1975;12:189–198. [PubMed: 1202204]
24. Jovicich J, Czanner S, Greve D, et al. Reliability in multi-site structural MRI studies: effects of gradient non-linearity correction on phantom and human data. *Neuroimage* 2006;30:436–443. [PubMed: 16300968]
25. Sled JG, Zijdenbos AP, Evans AC. A nonparametric method for automatic correction of intensity nonuniformity in MRI data. *IEEE Trans Med Imaging* 1998;17:87–97. [PubMed: 9617910]
26. Fischl B, Salat DH, Busa E, et al. Whole brain segmentation: automated labeling of neuroanatomical structures in the human brain. *Neuron* 2002;33:341–355. [PubMed: 11832223]
27. Makris N, Meyer JW, Bates JF, Yeterian EH, Kennedy DN, Caviness VS. MRI-Based topographic parcellation of human cerebral white matter and nuclei II. Rationale and applications with systematics of cerebral connectivity. *Neuroimage* 1999;9:18–45. [PubMed: 9918726]
28. Fischl B, van der Kouwe A, Destrieux C, et al. Automatically parcellating the human cerebral cortex. *Cereb Cortex* 2004;14:11–22. [PubMed: 14654453]
29. Dale AM, Sereno MI. Improved localization of cortical activity by combining EEG and MEG with MRI cortical surface reconstruction: a linear approach. *Journal of Cognitive Neuroscience* 1993;5:162–176.
30. Dale AM, Fischl B, Sereno MI. Cortical surface-based analysis. I. Segmentation and surface reconstruction. *Neuroimage* 1999;9:179–194. [PubMed: 9931268]
31. Fischl B, Dale AM. Measuring the thickness of the human cerebral cortex from magnetic resonance images. *Proc Natl Acad Sci U S A* 2000;97:11050–11055. [PubMed: 10984517]
32. Fischl B, Sereno MI, Dale AM. Cortical surface-based analysis. II: Inflation, flattening, and a surface-based coordinate system. *Neuroimage* 1999;9:195–207. [PubMed: 9931269]
33. Fischl B, Sereno MI, Tootell RB, Dale AM. High-resolution intersubject averaging and a coordinate system for the cortical surface. *Hum Brain Mapp* 1999;8:272–284. [PubMed: 10619420]
34. Salat DH, Buckner RL, Snyder AZ, et al. Thinning of the cerebral cortex in aging. *Cereb Cortex* 2004;14:721–730. [PubMed: 15054051]
35. Rosas HD, Liu AK, Hersch S, et al. Regional and progressive thinning of the cortical ribbon in Huntington's disease. *Neurology* 2002;58:695–701. [PubMed: 11889230]

36. Kuperberg GR, Broome MR, McGuire PK, et al. Regionally localized thinning of the cerebral cortex in schizophrenia. *Arch Gen Psychiatry* 2003;60:878–888. [PubMed: 12963669]
37. Desikan RS, Segonne F, Fischl B, et al. An automated labeling system for subdividing the human cerebral cortex on MRI scans into gyral based regions of interest. *Neuroimage* 2006;31:968–980. [PubMed: 16530430]
38. Walhovd KB, Fjell AM, Amlie I, et al. Multimodal imaging in mild cognitive impairment: Metabolism, morphometry and diffusion of the temporal-parietal memory network. *Neuroimage* 2009;45:215–223. [PubMed: 19056499]
39. Edison P, Archer HA, Hinz R, et al. Amyloid, hypometabolism, and cognition in Alzheimer disease: an [¹¹C]PIB and [¹⁸F]FDG PET study. *Neurology* 2007;68:501–508. [PubMed: 17065593]
40. Langbaum JB, Chen K, Lee W, et al. Categorical and correlational analyses of baseline fluorodeoxyglucose positron emission tomography images from the Alzheimer's Disease Neuroimaging Initiative (ADNI). *Neuroimage* 2009;45:1107–1116. [PubMed: 19349228]
41. Villain N, Desgranges B, Viader F, et al. Relationships between hippocampal atrophy, white matter disruption, and gray matter hypometabolism in Alzheimer's disease. *J Neurosci* 2008;28:6174–6181. [PubMed: 18550759]
42. Karas G, Sluimer J, Goekoop R, et al. Amnestic mild cognitive impairment: structural MR imaging findings predictive of conversion to Alzheimer disease. *AJNR Am J Neuroradiol* 2008;29:944–949. [PubMed: 18296551]
43. Devanand DP, Habeck CG, Tabert MH, et al. PET network abnormalities and cognitive decline in patients with mild cognitive impairment. *Neuropsychopharmacology* 2006;31:1327–1334. [PubMed: 16292330]
44. Minoshima S, Frey KA, Foster NL, Kuhl DE. Preserved pontine glucose metabolism in Alzheimer disease: a reference region for functional brain image (PET) analysis. *J Comput Assist Tomogr* 1995;19:541–547. [PubMed: 7622680]
45. Shaw LM, Korecka M, Clark CM, Lee VM-Y, Trojanowski JQ. Biomarkers of neurodegeneration for diagnosis and monitoring therapeutics. *Nature Reviews Drug Discovery* 2007;6:295–303.
46. Morris JC. The Clinical Dementia Rating (CDR): current version and scoring rules. *Neurology* 1993;43:2412–2414. [PubMed: 8232972]
47. Wechsler, D. *Wechsler Memory Scale - Revised*. Psychological Corporation; San Antonio, Texas: 1987.
48. Hanley JA, McNeil BJ. A method of comparing the areas under receiver operating characteristic curves derived from the same cases. *Radiology* 1983;148:839–843. [PubMed: 6878708]
49. Hansson O, Zetterberg H, Buchhave P, Londos E, Blennow K, Minthon L. Association between CSF biomarkers and incipient Alzheimer's disease in patients with mild cognitive impairment: a follow-up study. *Lancet Neurol* 2006;5:228–234. [PubMed: 16488378]
50. Hansson O, Buchhave P, Zetterberg H, Blennow K, Minthon L, Warkentin S. Combined rCBF and CSF biomarkers predict progression from mild cognitive impairment to Alzheimer's disease. *Neurobiol Aging* 2009;30:165–173. [PubMed: 17646035]
51. Sluimer JD, Bouwman FH, Vrenken H, et al. Whole-brain atrophy rate and CSF biomarker levels in MCI and AD: A longitudinal study. *Neurobiol Aging*. 2008
52. Shaw LM, Vanderstichele H, Knapik-Czajka M, et al. Cerebrospinal fluid biomarker signature in Alzheimer's disease neuroimaging initiative subjects. *Ann Neurol* 2009;65:403–413. [PubMed: 19296504]

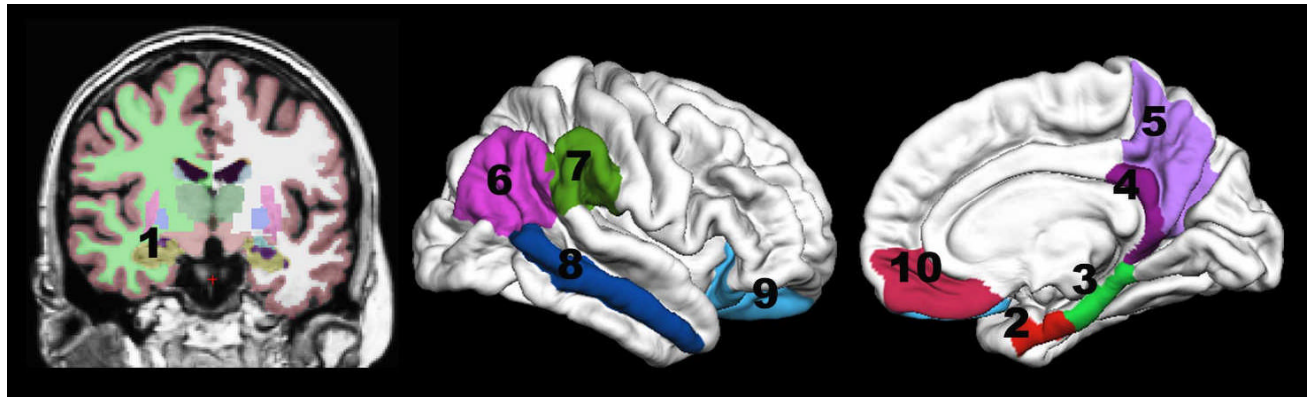
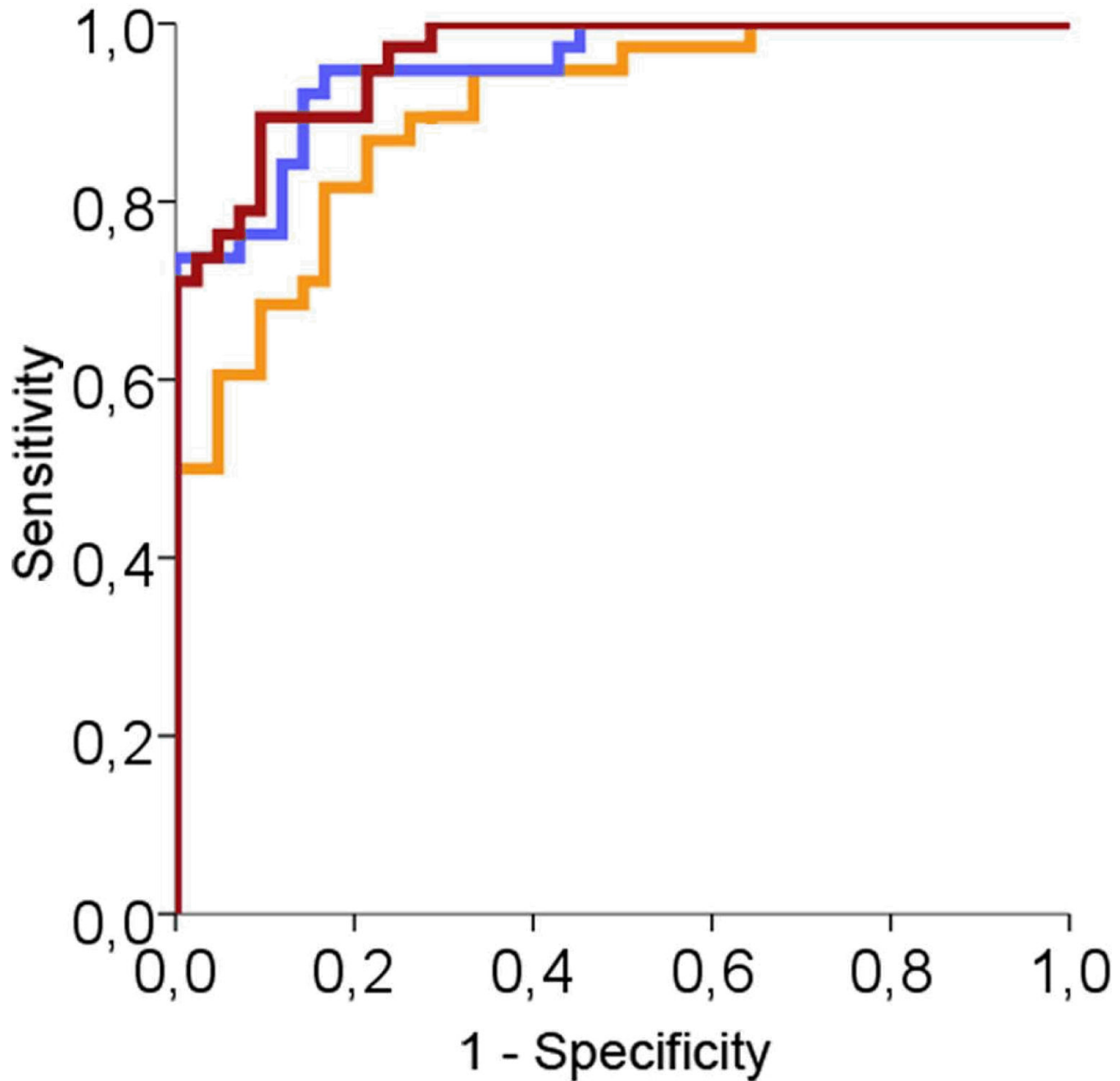
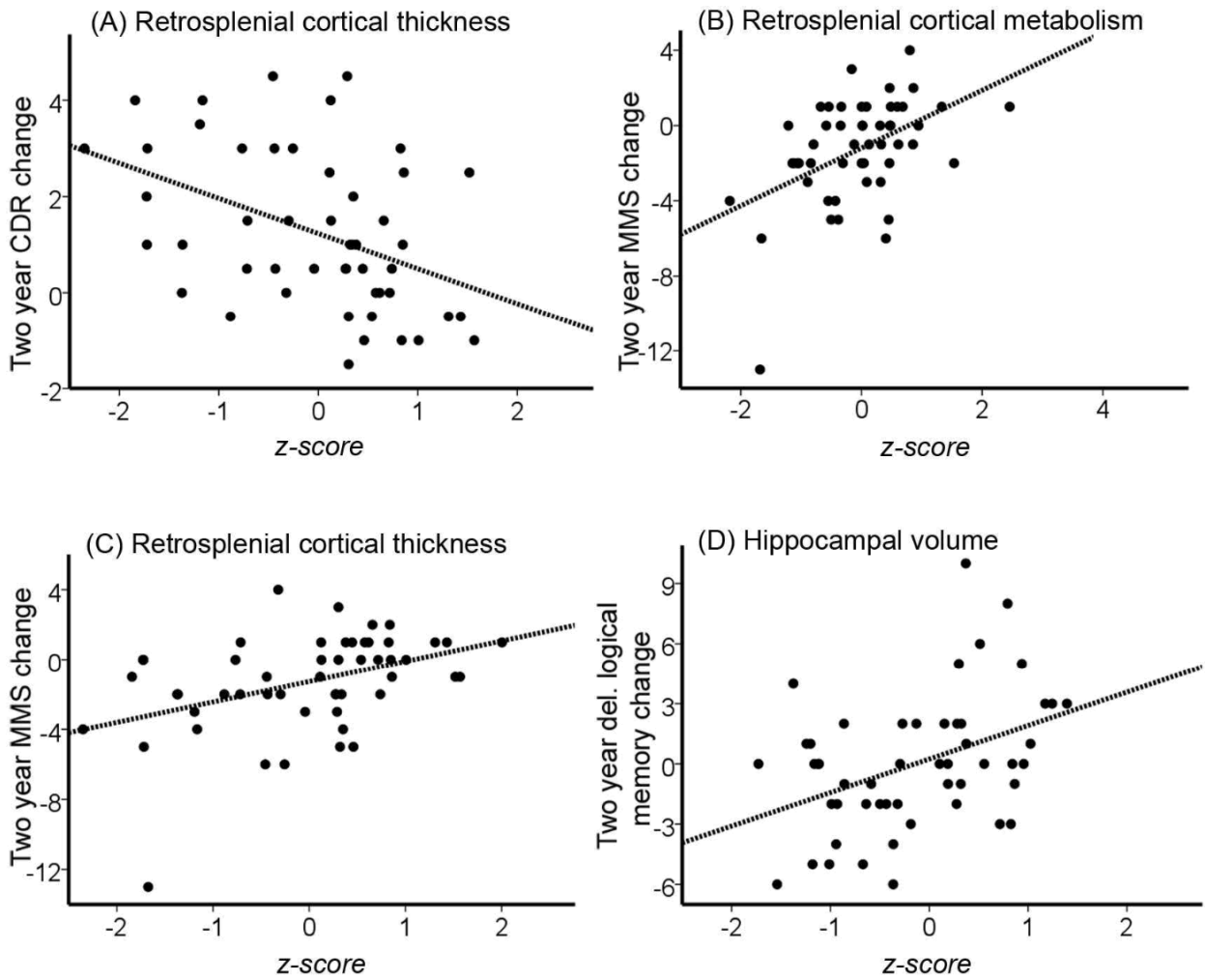


Figure 1.

The regions of interest used: 1) hippocampus, 2) entorhinal, 3) parahippocampal, 4) retrosplenial, 5) precuneus, 6) inferior parietal, 7) supramarginal, 8) middle temporal, 9) lateral orbitofrontal and 10) medial orbitofrontal cortices.

**Figure 2.**

Comparison of receiver operating characteristics (ROC) curves for using one, vs a combination of two and all three variables shown to be unique predictors of normal control vs Alzheimer's Disease classification. Yellow: predicted probability based on hippocampal volume alone, area under the curve (AUC): .900 (S.E. = .033). Blue: predicted probability based on hippocampal volume and t-tau/a β 42 ratio, AUC: .950 (S.E. = .022). Red: predicted probability based on hippocampal volume, t-tau/a β 42 ratio and retrosplenial cortical thickness, AUC: .961 (S.E. = .018).

**Figure 3.**

The regression plots for two year change scores in the Mild Cognitive Impairment (MCI) group significantly ($p < .05$) predicted from MR morphometry and PET metabolism variables A) Clinical Dementia Rating (CDR) change predicted from retrosplenial cortical thickness, Mini Mental Status Exam (MMSE) change predicted from B) retrosplenial cortical metabolism and C) retrosplenial cortical thickness, and D) Delayed Logical Memory change predicted from hippocampal volume.

Demographic characteristics of the three subsamples.

Table 1

| | NC N = 42,16 F / 26 M | | | | MCI N = 73,25 F / 48 M | | | | AD N = 38,16 F / 22 M | | | |
|------------------|--------------------------|-------|-------------|------|---------------------------|-------------|------|-------|--------------------------|--|--|--|
| | M | SD | Range | M | SD | Range | M | SD | Range | | | |
| Age | 75.5 | (5.4) | 62.2 – 84.7 | 74.5 | (7.0) | 55.5 – 88.9 | 76.2 | (7.5) | 58.8 – 88.1 | | | |
| Education | 16.0 | (3.2) | 8 – 20 | 16.0 | (2.9) | 8 – 20 | 14.3 | (3.6) | 4 – 20 | | | |
| MMSE | 29.1 | (1.0) | 26–30 | 27.0 | (1.7) | 24–30 | 23.8 | (2.0) | 20–26 | | | |
| MMSE_c | -0.2 | (1.6) | -4 – 3 | -1.3 | (2.8) | -13 – 4 | -5.2 | (5.8) | -22 – 4 | | | |
| CDR | 0.0 | (0.0) | 0 – 0 | 0.5 | (0.0) | 0.5 – 0.5 | 0.8 | (0.3) | 0.5 – 1.0 | | | |
| CDR_c | 0.2 | (0.7) | -0.5 – 3.5 | 1.2 | (1.6) | -1.5 – 4.5 | 4.0 | (3.1) | 0 – 11 | | | |
| LM-del | 12.0 | (3.6) | 6 – 22 | 4.1 | (2.7) | 0 – 8 | 1.1 | (2.0) | 0 – 8 | | | |
| LM-del_c | 1.2 | (4.1) | -10 – 8 | 0 | (3.3) | -6 – 10 | -0.7 | (1.1) | -4 – 1 | | | |

MMSE = Mini mental Status Exam, CDR = Clinical Dementia Rating, LM-del = delayed Logical Memory from the Wechsler Memory Scale. The numbers refer to baseline data, with the exception of MMSE_c, CDR_c, and LM-del_c, which refer to change across two years (baseline score subtracted from score at 2 year follow-up). MMSE and LM-del change scores were available for 36 NC, 51 MCI, and 25 AD. CDR sum of boxes change scores were available for 34 NC, 49 MCI, and 25 AD.

Results from logistic regression analyses for each method predicting NC vs AD.

Table 2

| Method | Step | Measure | B | P | Odds ratio | % Corr. Class. | R ² |
|--------|------|----------------------------|--------|------|------------|-----------------------------------|----------------|
| MR | 1 | Hippocampus | -.306 | .000 | | | |
| | 2 | Hippocampus | -2.291 | .000 | .101 | NC: 83.3 AD: 81.6 All: 82.5 | .601 |
| | | Retrosplenial cortex | -1.202 | .014 | .301 | | |
| | 3 | Hippocampus | -1.581 | .011 | .206 | NC: 88.1 AD: 78.9 All: 83.8 | .665 |
| | | Entorhinal cortex | -1.314 | .026 | .269 | | |
| | | Retrosplenial cortex | -1.230 | .024 | .292 | All: 85.0 | |
| PET | 1 | Entorhinal cortex | -1.627 | .000 | .197 | NC: 85.7 AD: 73.7 All: 80.0 | .461 |
| | 2 | Entorhinal cortex | -2.142 | .000 | .117 | | |
| | | Lateral orbitofrontal cor. | .675 | .048 | 1.964 | NC: 81.0 AD: 76.3 All: 78.8 | .506 |
| | 3 | Entorhinal cortex | -2.094 | .000 | .123 | NC: 88.1 AD: 76.3 All: 82.5 | .620 |
| | | Retrosplenial cortex | -1.866 | .003 | .155 | | |
| | | Lateral Orbitofrontal cor. | 1.701 | .002 | 5.481 | All: 81.2 | |
| CSF | 1 | T-tau/β42 | 2.775 | .000 | 16.036 | NC: 85.7 AD: 76.3 All: 81.2 | .523 |

R² is Nagelkerke R².

Results from the multimodal logistic regression analyses predicting NC vs AD.

Table 3

| Step | Measure | NC vs AD | | | | | R^2 |
|-----------|------------------------|----------|------|------------|---------------------------------------|------|-------|
| | | B | P | Odds ratio | % Corr. Class. | | |
| 1 | MR Hippocampus | -2.306 | .000 | .100 | NC: .83.3 AD: .81.6 All: .82.5 | .601 | |
| | T-tau/ $\alpha\beta42$ | 2.141 | .001 | 8.509 | NC: .88.1 AD: .81.6 All: .85.0 | | |
| 2 | MR Hippocampus | -2.029 | .000 | .132 | NC: .88.1 AD: .81.6 All: .85.0 | .733 | |
| | T-tau/ $\alpha\beta42$ | 2.141 | | 11.140 | NC: .90.5 AD: .86.8 All: .88.8 | | |
| 3 | MR Hippocampus | -1.861 | .002 | .155 | NC: .90.5 AD: .86.8 All: .88.8 | .778 | |
| | MR Retrosplenial | -1.239 | .028 | .290 | | | |
| | T-tau/ $\alpha\beta42$ | 2.411 | .002 | | | | |
| NC vs MCI | | | | | | | |
| 1 | MR Hippocampus | -1.360 | .000 | .257 | NC: .54.8 MCI: .80.8 All: .71.3 | .312 | |
| | T-tau/ $\alpha\beta42$ | 1.422 | .006 | 4.146 | MCI: .87.7 All: .79.1 | | |
| 2 | MR Hippocampus | -1.124 | .000 | .325 | NC: .64.3 MCI: .87.7 All: .79.1 | .399 | |
| | T-tau/ $\alpha\beta42$ | 1.422 | | | | | |

The variables explaining unique variance within each method, as listed in Table 2, were included in the set of predictor variables, i.e. for MR: hippocampal volume, retrosplenial, and entorhinal thickness, for PET: entorhinal, retrosplenial, and lateral orbitofrontal metabolism, and for CSF: the ratio of T-tau to Abeta 42. R^2 is Nagelkerke R^2 .

Table 4

Correlations between the predictor variables included in the regression models predicting NC/AD classification and the change in Clinical Dementia Rating (CDR) sum of boxes (n = 49) and MMSE (n = 51) scores across two years in the MCI group.

| | CDR sum of boxes change | MMSE change | Delayed Logical Memory change |
|------------------------|--------------------------------|--------------------|--------------------------------------|
| MR hippocampus | -.29 | .29 | .41 |
| MR Entorhinal | -.17 | .23 | .34 |
| MR Retrosplenial | -.43 | .42 | .35 |
| PET Entorhinal | -.30 | .38 | .28 |
| PET Retrosplenial | -.22 | .47 | .11 |
| PET Lat. Orbitofrontal | -.02 | .27 | -.05 |
| T-tau/αβ42 | .02 | .08 | -.23 |

Bold numbers indicate p < .05, corrected for seven comparisons.